RESEARCH ARTICLE

Feeding Performance of King Mackerel, *Scomberomorus Cavalla*

JOURNAL OF EXPERIMENTAL ZOOLOGY
PART A
ECOLOGICAL GENETICS AND PHYSIOLOGY
A Journal of Integrative Biology

AMBER R. FERGUSON[1]*, DANIEL R. HUBER[2], MARC J. LAJEUNESSE[1], AND PHILIP J. MOTTA[1]

[1]Department of Integrative Biology, University of South Florida, Tampa, Florida
[2]Department of Biology, University of Tampa, Tampa, Florida

ABSTRACT

Feeding performance is an organism's ability to capture and handle prey. Although bite force is a commonly used metric of feeding performance, other factors such as bite pressure and strike speed are also likely to affect prey capture. Therefore, this study investigated static bite force, dynamic speeds, and predator and prey forces resulting from ram strikes, as well as bite pressure of the king mackerel, *Scomberomorus cavalla*, in order to examine their relative contributions to overall feeding performance. Theoretical posterior bite force ranged from 14.0–318.7 N. Ram speed, recorded with a rod and reel incorporated with a line counter and video camera, ranged from 3.3–15.8B L/s. Impact forces on the prey ranged from 0.1–1.9 N. Bite pressure, estimated using theoretical bite forces at three gape angles and tooth cross-sectional areas, ranged from 1.7–56.9 MPa. Mass-specific bite force for king mackerel is relatively low in comparison with other bony fishes and sharks, with relatively little impact force applied to the prey during the strike. This suggests that king mackerel rely on high velocity chases and high bite pressure generated via sharp, laterally compressed teeth to maximize feeding performance. *J. Exp. Zool. 9999A: XX–XX, 2015.* © 2015 Wiley Periodicals, Inc.

J. Exp. Zool. 9999A:1–15, 2015

How to cite this article: Ferguson AR, Huber DR, Lajeunesse MJ, Motta PJ. 2015. Feeding Performance of King Mackerel, *Scomberomorus Cavalla*. J. Exp. Zool. 9999:1–15.

INTRODUCTION

Feeding performance, the ability to successfully capture and handle prey (Wainwright, '88, '91; Van Wassenbergh et al., 2007; Habegger et al., 2010), is dependent upon a variety of sensory and musculoskeletal processes. Predators must first locate potential prey items using olfactory, visual, electrical, and hydrodynamic stimuli (Shashar et al., 2000; Pohlmann et al., 2001; Stewart et al., 2013), after which a successful strike must be initiated. Strikes may involve significant contribution of the locomotor system, as is the case in ram feeders such as the great barracuda, *Sphyraena barracuda*, which capture prey by striking at high velocity (Grubich et al., 2008; Porter and Motta, 2004). Alternatively, locomotion may make little contribution to the strike, as exemplified by suction feeders such as the sunfishes, family Centrarchidae, which generate negative pressures within the oropharyngeal cavity to draw water and prey into the mouth (Lauder, '80; Wainwright et al., 2001; Higham et al., 2005). Once prey is acquired, it generally must be processed, depending on prey size and mechanical properties, within the oropharyngeal cavity via biting prior to deglutition (Huber et al., 2005; Grubich et al., 2008; Mara et al., 2009; Whitenack and Motta, 2010; Erickson et al., 2012). While it is apparent that acquiring food involves the coordinated performance of sensory, locomotive, and feeding mechanisms, feeding studies have generally examined only individual performance parameters at a time. The simultaneous examination of multiple performance parameters will likely yield

Conflicts of interest: None.
*Correspondence to: Amber R. Ferguson, Department of Integrative Biology, University of South Florida, Tampa, FL, 33620.
E-mail: arf@mail.usf.edu
Received 1 December 2014; Revised 5 March 2015; Accepted 6 March 2015
DOI: 10.1002/jez.1933
Published online XX Month Year in Wiley Online Library (wileyonlinelibrary.com).

insight into the complex interaction between predator and prey (Rice and Westneat, 2005).

One of the more commonly assessed metrics of feeding performance is bite force, which is the emergent product of the morphology of the cranium and jaws, and physiology, architecture, and leverage of the jaw muscles (Herrel et al., 2001; Huber et al., 2005; Habegger et al., 2010). Bite force has been shown to affect resource partitioning and dietary diversity, with those species consuming hard prey having above average mass-specific bite forces (Wainwright, '88; Herrel et al., 2001; Huber et al., 2005; Herrel and Holanova, 2008; Mara et al., 2009; Schaerlaeken et al., 2012). Furthermore, ontogenetic studies have found that small and/or durophagous species exhibit positive allometry of bite force, which may allow those animals access to functionally difficult resources earlier in life than organisms with isometric ontogenetic trajectories (Habegger et al., 2012; Kolmann et al., 2009).

While significant relationships between morphology, behavior, and ecology have been found with regard to bite force, most of the studies on this topic have either focused on durophagous species (Hernandez and Motta, '97; Huber et al., 2005; Kolmann et al., 2009), for which high bite forces are a prerequisite for the occupation of their ecological niche, or have neglected the role of the teeth in feeding performance (but see Herrel et al., 2001; Erickson et al., 2003 Erickson et al., 2012). Bite pressure, resulting from bite force applied over tooth contact area, is an often-neglected aspect of feeding performance complicated by a lack of knowledge regarding the number of teeth in contact with the prey, how tooth contact area changes during tooth puncture, and how gape angle changes, consequently altering the bite force that drives tooth pressure (Gidmark et al., 2013; Whitenack and Motta, 2010). Some ram feeding fish such as the great barracuda, *Sphyraena barracuda*, have relatively low bite force (Habegger et al., 2010) but have very sharp teeth (Porter and Motta, 2004; Habegger et al., 2010). Consequently, the pressures generated by these teeth alleviate the need for high bite forces when feeding on soft-bodied prey. This relationship between tooth geometry and bite force is reversed for durophagous species such as the horn shark, *Heterodontus francisci* which use high bite forces and molariform teeth to crush hard prey (Hernandez and Motta, '97; Korff and Wainwright, 2004; Huber et al., 2005). Erickson et al. (2012) investigated the bite pressure generated by the caniform and molariform teeth of 23 species of extant crocodilians during prey capture and processing, and found higher bite pressures in piscivorous species with sharper teeth despite lower bite forces. Sharper and more pointed teeth may reduce the selection pressure for predators to develop high bite forces, with those species exhibiting rapid replacement of sharp teeth potentially exemplifying this relationship (Wroe et al., 2008; Habegger et al., 2010; Whitenack et al., 2011). Another component to maintaining sharp teeth could be drag reduction in fast swimmers. A high bite force requires large heads as space for muscles is needed (Herrel et al., 2001; Lailvaux et al., 2004, Habegger et al., 2012), while in fast species such as king mackerel, *Somberomorus cavalla*, large heads may be selected against. An alternative to having high bite forces may be to have a streamlined body and sharp cutting teeth. Thus, it is apparent that bite force does not tell the entire story regarding feeding performance in ecological niches that have differing demands.

Like bite pressure, strike kinematics are another aspect of organismal performance that affects prey capture success, yet has received little attention in feeding studies until recently (see Norton, 1991; Porter and Motta, 2004, Holzman et al., 2012). Many studies have examined fish swimming speeds (Bainbridge, 1959; Videler and Hess, '84; McCormick and Molony, '93; Bernal et al., 2001), yet the extent to which the impact generated during predator-prey contact affects the ability to disable prey is unknown. High velocity strikes such as those utilized by ram feeding fish transfer momentum to prey items, thereby accelerating them. The effect of the resultant force may contribute significantly to prey capture success, especially for sharp-toothed predators in which the impact may generate tooth pressures that cause puncture independent of the applied bite force. Because it is a dynamic interaction, when the predator strikes prey such as small fish, only a fraction of the predator's force is applied to the prey due to the mass differential between predator and prey; the remaining force is applied to the environment.

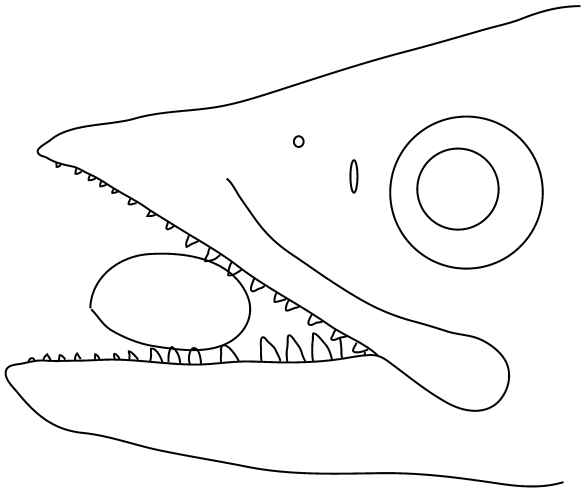

Figure 1. Illustration, taken from a photograph, of prey (Spanish sardine, *Sardinella aurita*) being bitten by a king mackerel, *Scomberomorus cavalla*. Teeth in contact with the prey were used for calculation of bite pressure. Calculations were made from anterior to posterior teeth for four consecutive teeth; this diagram depicts a representative position with the prey at a middle position along the lower jaw with the tooth tips contacting it.

Figure 2. Cut marks on (A) a recovered prey from a failed strike matches those made by (B) a simulated strike on a similarly sized prey in the laboratory using the teeth of a king mackerel, *Scomberomorus cavalla*, of the same size. The spacing of the cut marks indicates that the posterior teeth contact prey first (i.e., the predator strikes with mouth open) because penetration of the anterior teeth would result in cut marks spaced more closely together.

The purpose of this study was to examine the bite force, predator and prey impact force, and tooth pressure generated during feeding events in the ram-feeding king mackerel, *Scomberomorus cavalla* (Cuvier, 1828). King mackerel are coastal pelagic predatory fishes that are found along the Atlantic coast from North Carolina to Brazil, including the Gulf of Mexico. These fish have sharp, non-serrated, laterally compressed teeth (Morgan and King, '83), suited for cutting soft-bodied prey (Wall et al., 2009). Top swimming speeds of king mackerel are unknown, but other mackerel species such as the Atlantic mackerel, *Scomber scombrus*, may attain burst speeds of up to 11 body lengths per second (bl/s) (Videler and Hess, '84). In order to investigate the hypothesis that predator force and tooth pressure play an important role in the prey capture success of king mackerel, *Scomberomorus cavalla*, this study: (1) described the musculature used in generating bite force, (2) calculated maximal theoretical static bite force at three gape angles and the scaling relationships of bite force with respect to body length, (3) calculated the dynamic predator and prey forces that occur during predator-prey impact, and (4) estimated bite pressure exerted on the prey during tooth penetration. By examining bite force, predator force and tooth pressure, this study aims to provide a more holistic, quantitative, perspective on prey capture performance in ram feeding fishes.

MATERIALS AND METHODS

Specimen Collection for Theoretical Bite Force

King mackerel, *Scomberomorus cavalla* (Cuvier, 1828) were collected by hook and line in the Gulf of Mexico off Madeira Beach, Florida by recreational fishers. Fork length (FL, measured from tip of the jaw with mouth closed to the center of the tail fork), total length (TL, measured from the tip of the jaw with mouth closed to the furthest tip of the tail), and weight were measured. Weight was estimated using a length-weight regression (SEDAR, 2009) when weight was unable to be directly determined. Heads were removed

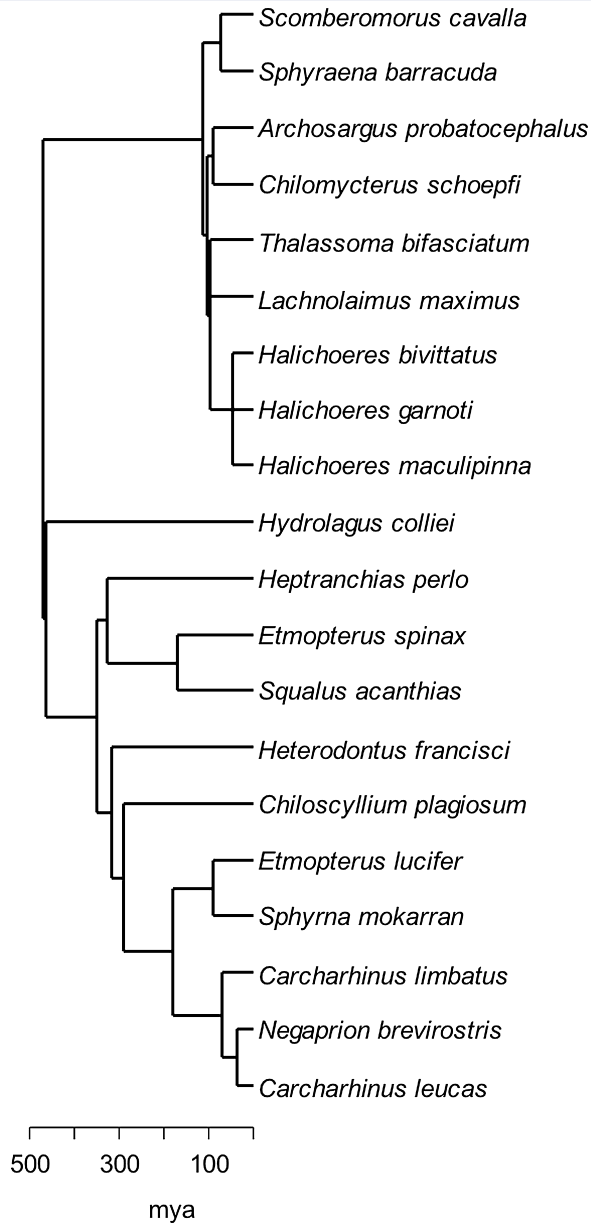

Figure 3. The phylogenetic relationships among 20 species of teleost fishes and sharks. Topology was based on Betancur et al. (2013) and Vélez-Zuazo and Agnarsson (2011), and internode branch-lengths were based on known divergence times reported by Betancur et al. (2013) and Heinicke et al. (2009).

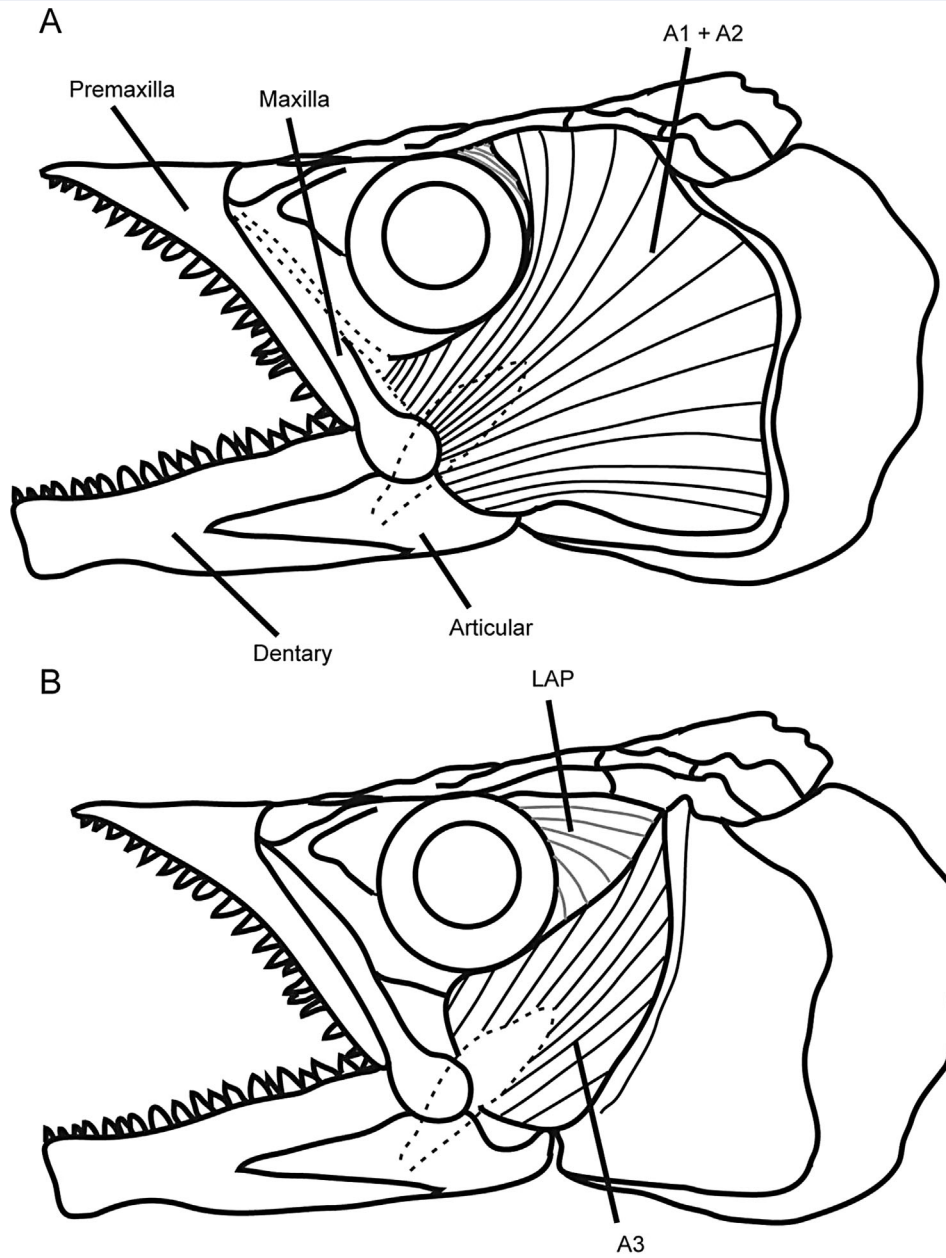

Figure 4. Jaw closing musculature of the king mackerel, *Scomberomorus cavalla*. (A) The Adductor mandibulae 1 and 2 (A1 + A2) muscle is the most superficial fan shaped muscle. (B) The adductor mandibulae 3 (A3) is deep to the A1A2 complex and overlaps the levator arcus palatini (LAP) muscle. The lacrimal bone is removed.

and frozen until dissections were performed (muscle nomenclature was based on Winterbottom, 1974).

Bite Force

Theoretical bite force was calculated for 23 fresh-frozen fish, sex undetermined, ranging from 63.2 cm to 117.8 cm FL, following the three-dimensional static equilibrium model used by Huber et al. (2005). Only force contributed by the lower jaw was considered, as the upper jaw is non-protrusible, and force contributed by the upper jaw would be a reaction to prey being driven into the upper jaw by the lower jaw. The adductor mandibulae divisions (A1, A2, A3) were modeled as a single

Table 1. Absolute values of anterior and posterior bite force (N) for king mackerel, *Scomberormorus cavalla* (n = 23) with respect to fork length (cm) was calculated at three different gape angles, 0% maximum gape (mouth closed), 50% maximum gape (mouth half open), and 100% maximum gape (mouth maximally open).

	Anterior			Posterior		
FL (cm)	0%	50%	100%	0%	50%	100%
63.2	11.4	8.0	9.2	53.1	36.6	23.3
69.6	9.7	5.1	10.9	50.8	33.4	18.9
72.8	13.5	15.6	11.9	70.6	58.9	53.7
76.5	21.0	10.5	11.0	100.7	44.4	34.8
79.1	19.4	14.2	20.6	95.1	96.4	44.8
79.4	5.6	5.7	8.6	31.4	41.6	20.8
80.9	14.1	8.5	8.3	93.4	39.5	40.4
81.2	5.1	3.8	5.9	27.3	25.5	14.0
84.0	19.7	15.8	19.6	93.9	66.7	50.1
84.9	30.4	16.0	21.2	137.7	84.2	53.0
86.0	16.8	7.8	14.2	77.8	55.6	27.3
86.9	19.1	17.9	15.1	92.9	65.2	58.8
87.0	17.3	10.2	12.4	90.9	51.9	39.4
88.0	17.7	13.7	17.9	76.7	66.6	45.4
89.2	20.2	17.7	16.9	85.0	59.5	57.9
90.0	28.3	13.7	21.3	136.4	85.4	54.1
92.9	23.1	17.0	24.2	111.6	96.0	57.6
93.8	27.8	18.6	15.6	132.3	55.9	51.8
98.6	19.6	9.7	11.6	98.7	48.7	30.9
104.0	32.9	43.6	35.2	154.0	153.1	122.6
107.0	39.2	22.0	25.4	193.8	92.4	122.6
114.2	70.5	30.8	21.3	318.7	81.6	104.4
117.8	44.6	53.6	33.3	209.8	134.8	154.2

muscle because of a common fiber direction, insertion, and line of action. This model may underestimate peak bite forces and affect measurements of force at multiple gapes, however the error caused by shredding of the muscle divisions when removed separately is likely great. The muscle was removed and bisected through its center of mass, perpendicular to its principal fiber direction. To determine the center of mass the muscle was suspended from a string at two different points, and each time a line was traced along the string. Center of mass was the point where the two lines intersected. Photos of the cross sections were taken and anatomical cross sectional area (CSA) was measured using NIH Image J software (ImageJ64 v.1.42q, National Institute of Health, Bethesda, MD, USA). CSA was used instead of physiological cross sectional area due to the fibers being parallel (fiber angle $\sim 0°$) near the insertion of the muscle and at its center of mass, despite the fact that fibers diverged from parallel to accommodate the eye dorsally. Position of the origin and insertion of the adductor mandibulae complex, anterior and posterior bite points (dorsal surface of the mandibular symphysis and last tooth near the jaw joint, respectively), and jaw joint were obtained using a three-dimensional digitizer (Polhemus, Colchester, VT, USA). The maximum theoretical tetanic output (P_0) of the adductor musculature was calculated by multiplying CSA by the specific tension (T_S) of fish muscle ($25\,Ncm^{-2}$; Van Wassenbergh et al., 2007).

$$P_0 = CSA \times T_S$$

Anterior and posterior bite forces (ABF and PBF respectively) were modeled via a 3D static equilibrium analysis in Mathcad (11.1, Mathsoft, Inc., Cambridge, MA, USA), and bite force was calculated with the following equation:

$$\Sigma F_{LJ} = F_{JR} + F_{AM} + F_B = 0$$

Where F_{LJ} is the force on the lower jaw, F_{JR} is the jaw joint reaction force, F_{AM} is the force generated by the adductor musculature, and F_B is the bite reaction force of the prey.

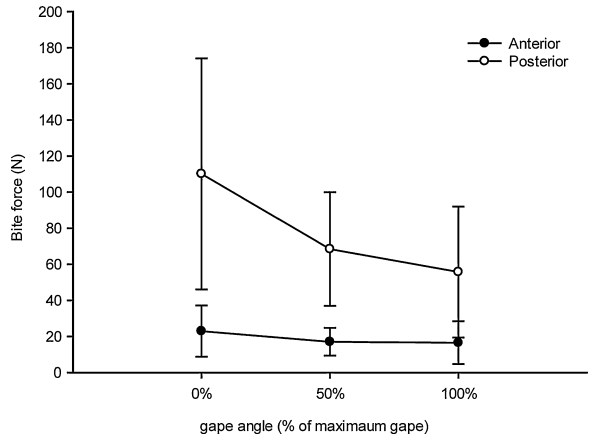

Figure 5. Bite force (N) of king mackerel, *Scomberomorus cavalla*, at 0% (mouth closed), 50% (mouth half open) and 100% (mouth fully open) maximum gape. Closed circles represent anterior bite force values and open circles represent posterior bite force values. Error bars are one standard deviation from the average.

Theoretical bite force was calculated with the jaw closed (0% maximum gape), half open (50% maximum gape), and maximally open (100% maximum gape). Mechanical advantage (MA) was calculated for all individuals at the three gape angles for both anterior and posterior bite positions. MA is the ratio of the force in-lever (distance from the muscle insertion to the jaw joint) divided by the force out-lever (distance from the bite point to the jaw joint), which were calculated using the 3D coordinates of the respective points.

Electrically stimulated tetanic bite force values were measured on a subset of six fish to validate theoretical estimates. Fish were caught using a rod and reel with an analog line counter (Diawa Saltist STTLW50LCA, Cypress, CA, USA) and a mounted GoPro Hero 2 or GoPro Hero 3 HD camera (120 fps and 240 fps, respectively) focused on the line counter. Lines were baited with frozen-thawed Spanish sardines, *Sardinella aurita*, live blue runner, *Caranx crysos*, or live mackerel scad, *Decapterus macarellus*. Fish were caught and immediately euthanized with an overdose of a 0.2% tricaine methanesulfate (MS 222) solution buffered with sodium bicarbonate by spraying the solution onto the gills. The adductor mandibulae (bilateral) divisions were stimulated wholly for approximately two seconds (30V, 60Hz, 0.02ms delay, 3ms pulse length) with a SD9 stimulator (Grass Telefactor, Quincy, MA, USA) by implanting two pairs of stainless steel hypodermic needles ~2.5 cm apart through each cheek into the adductor mandibulae complex. A piezoelectric load cell with custom lever arms (PCB Piezotronics 201B02) was placed between the anterior teeth (approximately 30% maximum gape) during stimulation of the anesthetized fish. Data were

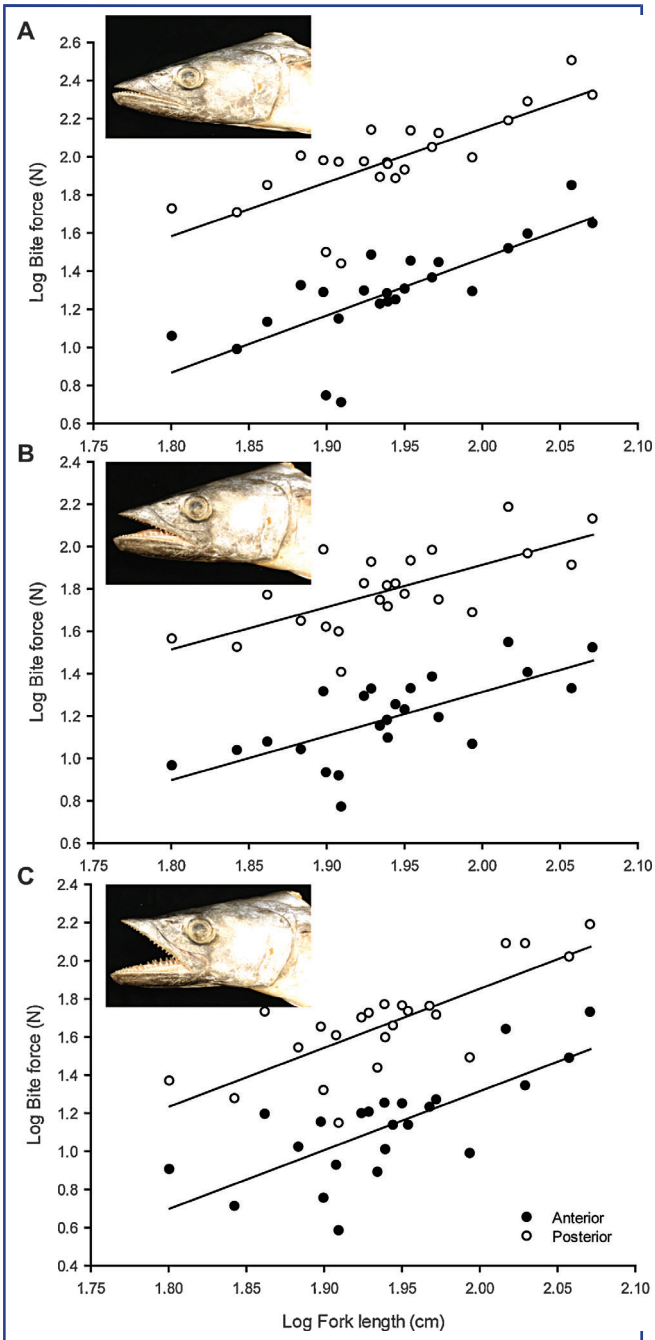

Figure 6. Log-transformed theoretical bite force (N) with respect to log-transformed fork length (cm) at (A) 0% maximum gape (mouth closed) (Log ABF = 3.0 × Log FL −4.5; Log PBF = 2.8 × Log FL −3.5), (B) 50% maximum gape (mouth half open) (Log ABF = 2.1 × Log FL −2.8; Log PBF = 2.0 × Log FL −2.1) and (C) 100% maximum gape, mouth fully open (Log ABF = 3.1 × Log FL −4.9; Log PBF = 3.1 Log FL −4.3), all of which scaled with isometry. Closed circles represent anterior bite force (ABF) and open circles represent posterior bite force (PBF).

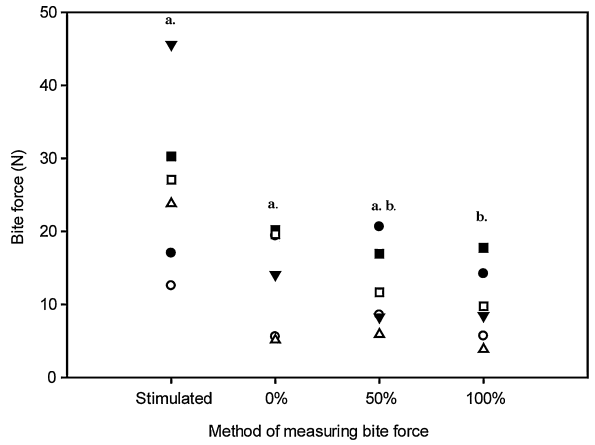

Figure 7. Bite forces of king mackerel, *Scomberomorus cavalla* (n = 6), from tetanic stimulation of the jaw adductor musculature and calculations of theoretical anterior bite force for the same individuals at 0% maximal gape (mouth closed), 50% maximum gape (mouth half open), and 100% maximal gape (mouth maximally open). Stimulated bite force (at approximately 30% maximum gape) was not significantly different than theoretical bite force at 0% maximum gape ($P > 0.05$) and 50% maximum gape ($P > 0.05$), but greater than theoretical bite force at 100% maximal gape ($P < 0.05$). Each individual is represented by one of the six symbols. Letters indicate values that are not significantly different.

acquired with a 6020E data acquisition board and LabVIEW 6.0 software (National Instruments Corp., Austin, TX, USA). This procedure was repeated 2–3 times per individual, with 1-3 minutes of rest between trials, and the largest value was recorded as maximal bite force.

Strike Dynamics

Seven king mackerel were caught as above (see Bite Force), using braided fishing line (Power Pro Depth Hunter 30 lb) to minimize stretching and reel drag set as low as possible so as to not limit strike speed of the fish or cause the line to free spool or tangle. Boat speed at the time of capture was recorded with a GPS (Magellan Explorist 210, Santa Clara, CA, USA) and subsequently subtracted from strike speed (see below). A strike was measured when a king mackerel struck a baitfish and swam away from the boat. Videos of the line counter were digitized using GoPro Cineform Studio Version1.2 to quantify the distance travelled by the line throughout the strike per unit time. These data were in turn fitted with an nth (5, 6, or 7) order polynomial that was numerically derived to ascertain line velocity and acceleration. The order of the polynomial was chosen for best fit by Student's paired t-test comparing data points from the digitized GoPro video (distance by time plot) and the same points from the calculated polynomial curves. The best fit curve had the lowest t value. The velocity and acceleration of the fishing line was assumed to be the same as the prey fish and the hooked king mackerel, and was used as a proxy for potential strike speed when the predator hit the prey. As the hook was attached to the prey during capture, the initial maximal acceleration measured is the acceleration of the predator and prey immediately after the impact occurred.

The amount of force required to stop the king mackerel from forward acceleration is equivalent to the maximum force the king mackerel is capable of exerting on the environment. This predator force was calculated as the negative of the mass of the predator, multiplied by the acceleration of the predator and prey fish throughout the strike:

$$F_{Pd} = -(m_k \times a_k)$$

where F_{Pd} is the predator force the king mackerel is capable of exerting on the environment during forward motion, m_k is the mass of the king mackerel, and a_k is the acceleration of the king mackerel and captured prey from the strike until it reached a maximum velocity. Prey force, the amount of force applied to the prey during forward acceleration of the prey, was estimated using Newton's second law of motion:

$$F_{Py} = m_{py} \times a_{py}$$

where F_{Py} is the prey force, m_{py} is the mass of the prey and a_{py} is the acceleration of the prey.

It is evident that not all available forward force is applied to the prey during capture due to the equivalent acceleration of predator and prey, yet considerably different mass.

Predator and prey forces were calculated assuming that the motion of the king mackerel toward the prey item was only in one plane, that the prey is motionless at the time of impact, and that the fishing line does not stretch. Skin friction drag on the fishing line was determined by trailing three lengths of line (30, 45, and 60 m) from a Rapala digital scale (RGSDS-50, Finland) behind the boat moving at an average trolling speed of 0.9 m/s. The forces created by drag on the fishing line alone were 0.3N, 0.3N, and 0.6N for lengths of line at 30, 45, and 60 m, respectively.

Bite Pressure

Bite pressure was calculated using teeth from the lower jaws of three fish (small: FL = 70 cm; medium: FL = 88 cm; large: FL = 107 cm) using the assumption that four teeth from each half of the lower jaw (8 teeth total) contact the prey at the same time during biting, based on the observation of failed prey captures on Spanish sardines (Fig. 1). Only lower jaw teeth were considered, as this was assumed to be a static system in which the upper jaw and lower jaw would be mirror images of force and pressure production. Pressure was measured from the most

Table 2. Results of strike dynamics experiments for king mackerel, *Scomberomorus cavalla* (n = 7). Mass of each fish is expressed in kilograms (kg), the table is ordered by increasing mass. Fork length (FL) of each fish is expressed in centimeters (cm). Maximum velocity for each fish is expressed in body lengths per second (bl/s). Maximum acceleration of each fish is expressed in m/s^2. Prey force is the force actually exerted on the prey, and is expressed in Newtons (N). Predator force is the maximum force the king mackerel is capable of exerting on the environment in the forward direction and is expressed in Newtons (N).

Mass (kg)	FL (cm)	Max velocity (bl/s)	Max acceleration (m/s^2)	Prey force (N)	Predator force (N)
3.4	76.5	13.6	11.5	1.7	39.7
3.8	79.1	5.0	1.4	0.2	5.5
3.9	79.4	9.4	9.1	1.4	35.0
4.1	81.9	3.3	0.5	0.1	2.1
4.1	81.2	15.8	7.6	1.1	31.4
4.3	82.0	8.8	12.8	1.9	54.6
7.4	98.6	3.7	11.0	1.7	81.6

anterior teeth to the most posterior teeth in consecutive increments of four teeth (e.g., 1–4, 2–5, etc.). Following this, all teeth were separated at their bases using a Dremel tool and indented orthogonally into modeling clay at 10%, 50%, and 100% of crown height to correspond with bite forces calculated for 100%, 50%, and 0% of max gape, respectively. A minimum distance of 10% penetration was chosen to represent the tooth tip because measurement of cross-sectional area of the exact tooth tip is imprecise (Erickson et al., 2012). Consequently, puncture pressure of the tooth tip is an underestimate. Depth of tooth penetration determined which gape angle value of theoretical bite force was used (10% penetration = 100% Maximum gape; 50% penetration = 50% maximum gape; 100% penetration = 0% maximum gape). The maximally open position of the jaw was used in the calculations for maximum bite pressure as the observation of failed strikes on Spanish sardines suggests the king mackerel strike the prey with the mouth fully open. This was evidenced from tooth puncture spacing on recovered prey, which matched that of the most posterior teeth of the king mackerel (Fig. 2.). Consequently, anterior bite pressure values were conservative, as the jaw would, in reality, be less than 100% maximally open when the tips of the teeth penetrate (see Results). Photos of the tooth indentations in the clay were taken, and the cross sectional area was measured using NIH Image J software (ImageJ64 v.1.42q, National Institute of Health, Bethesda, MD, USA). Theoretical bite force was calculated along the length of the lower jaw (as above), after which the theoretical bite force corresponding to tooth depth was averaged over the four penetrating teeth and divided by the cross sectional areas of the penetrating teeth to obtain the penetration pressure of the four teeth (Fig. 1).

All experimental procedures were approved by the Institutional Animal Care and Use Committee (IACUC) protocols W IS00000002 and T IS00000021 of the University of South Florida.

Statistical Analysis

Data was tested for normality using the Shapiro Wilk test, and homoscedasticity using the Bartlett test. Student's paired t-test was used to compare stimulated and calculated theoretical anterior bite force values for the same six individuals. Scaling of theoretical bite force was analyzed at all three gape angles and at both the anterior and posterior bite points for the available size range of fish. Theoretical bite force, jaw muscle cross sectional area, and mechanical advantage were log transformed and linear regressed using least-squares regression against log fork length for the three different gape angles in order to assess scaling relationships of bite force. Least squares regression was used as the error in the dependent variable is expected to be much higher than the error in the independent variable. 95% confidence intervals were compared to the isometric slope of 2 to determine allometric relationships of bite force and adductor CSA to body length, and an isometric slope of 0 for mechanical advantage. A comparison was not made between prey force, predator force and stimulated bite force due to a lack of overlapping individuals within these data sets. Bite force was linearly regressed against gape angle to determine if bite force changed with the position of the lower jaw. In order to compare the maximal anterior bite force of *Scomberomorus cavalla* to that of 19 other fish species, $\log_e$ anterior bite forces were linearly regressed using least-squares regression against $\log_e$ fish mass and studentized residuals were compared. To control for the phylogenetic history of these fish (Lajeunesse and Fox, 2015), anterior bite force data were size-corrected using the phylogenetic residuals based on Revell (2009) and implemented in the R package *phytools* (Revell, 2012). Phylogenetic generalized least squares (PGLS) regression was also used assuming trait evolution via Brownian motion. The PGLS analysis was completed with the gls() function from the *nlme* package (Pinheiro et al., 2015) assuming a maximum likelihood estimator (ML), and a Brownian correlation structure

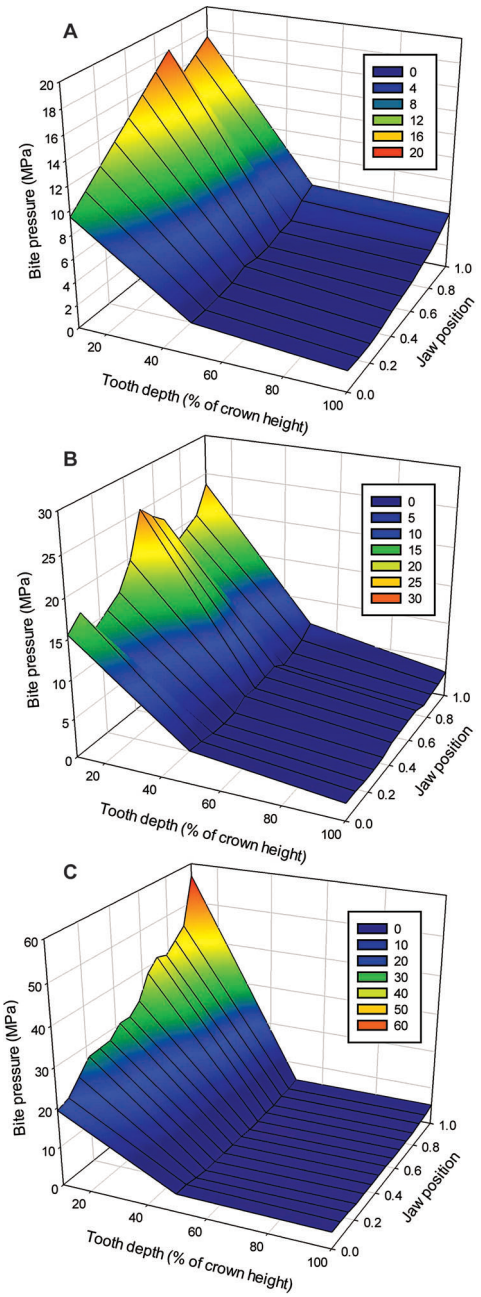

Figure 8. Bite pressure, tooth indentation depth, and position of prey along the jaw for a small (A) (FL = 70 cm, 2.6 kg), medium (B) (FL = 88 cm, 5.3 kg), and large (C) (FL = 107 cm, 9.5 kg) king mackerel, *Scomberomorus cavalla*. Teeth were indented at the tip of the tooth (10% of crown height), half of the tooth (50% of crown height), and the entire tooth (100% of crown height) representing 0%, 50%, and 100% mouth closure. Jaw position refers to the position of the prey along the lower jaw. The most anterior tooth was assigned the position 0.0 and the most posterior tooth was assigned the position 1.0.

defined by the corBrownian() function from the *ape* R package (Paradis et al., 2004). To quantify the amount of variability explained by the PGLS model we used McFadden's pseudo-r^2 (see Veall and Zimmermann, '96). The topology of our composite phylogeny (Fig. 3) of the 20 fish species was constructed using the bony fish tree from Betancur et al. (2013) and cartilaginous fishes following Vélez-Zuazo and Agnarsson (2011). Branch-length distances (in mya) were based on Betancur et al. (2013) and Heinicke et al. (2009). Bite pressure was linearly regressed using least-squares regression against distance along the jaw and indentation depth. Each regression was tested for significance using Analysis of Variance (ANOVA). All analyses were performed using R statistical software (R Foundation for Statistical Computing, Vienna, Austria).

RESULTS

Anatomy

The adductor mandibulae of king mackerel is made up of the A1, A2, A3, and Aw subdivisions (Fig. 4). The most superficial subdivisions, A1 and A2, make up a fan shaped muscle complex originating on the pterotic, frontal and preopercular bones. The A1–A2 complex inserts via a tendonous sheath extending from the maxilla to the Meckelian fossa and articular. Deep to the A1–A2 complex, the A3 subdivision is parallel fibered and originates on the hyomandibula, metapterygoid, quadrate, and preopercle (Fig. 4). The tendons of the A1–A2 complex and A3 subdivision fuse into a single tendon, that inserts into the Meckelian fossa and on the articular. The Aw subdivision is a bipennate muscle that lies within the Meckelian fossa on the medial face of the dentary, inserting on the medial side of the quadrate and preopercle, and originating on the dentary and articular.

Bite Force

Anterior mechanical advantage (MA) was 0.18 ± 0.04, 0.20 ± 0.05, and 0.21 ± 0.06 at 0%, 50%, and 100% maximum gape respectively, while posterior mechanical advantage was 0.62 ± 0.13, 0.77 ± 0.25, and 0.71 ± 0.25 at these gapes respectively. Theoretical *absolute* anterior bite force ranged from 5.1–70.5 N at 0% maximum gape, 3.8–53.6 N at 50%, and 5.9–33.3–N at 100%. Posterior bite force ranged from 27.3–318.7 N at 0% maximum gape, 25.5–153.1 N at 50%, and 14.0–154.2 N at 100% gape (Table 1). Bite forces were inversely proportional to gape angle ($P < 0.001$, Fig. 5), with *average* bite force highest at 0% maximum gape (anterior = 22.9 N ± 14.2 SD, posterior 110.1N ± 64.0 SD), decreasing at 50% maximum gape (anterior = 17.0N ± 7.7 SD, posterior = 68.4N ± 31.5 SD), and being lowest at 100% maximum gape (anterior = 16.5N ± 11.9 SD, posterior = 55.7N ± 36.3 SD). Bite force scaled isometrically with respect to body size at all three gape angles (Fig. 6). Cross sectional area of the adductor mandibulae complex scaled with positive allometry (b = 2.4, 95%CI 2.1–2.7). Mechanical advantaged scaled

Table 3. Bite pressure (MPa) values of a small (FL = 70 cm, 2.6 kg), medium (FL = 88 cm, 5.3 kg), and large (FL = 107 cm, 9.5 kg) king mackerel, Scomberomorus cavalla. Jaw position refers to the position of the prey along the lower jaw. The most anterior tooth was assigned the position 0.0 and the most posterior tooth was assigned the position 1.0. The number of measurement increments of four consecutive teeth per fish determined the number of jaw positions, thus there are more position in the larger fish. Larger fish have more tooth positions because of a larger total number of teeth along the lower jaw. Bite pressure values are reported in MPa for tooth penetration values of 10% (tip of tooth penetrating), 50% (half of tooth penetrating), and 100% (whole tooth penetrating) of tooth crown height.

Small				Medium				Large			
Jaw position	10%	50%	100%	Jaw position	10%	50%	100%	Jaw position	10%	50%	100%
1.00	17.4	5.3	4.9	1.00	23.6	6.6	3.3	1.00	56.9	5.1	5.2
0.90	16.4	4.7	4.1	0.92	20.2	5.4	2.8	0.93	44.9	4.5	4.5
0.80	15.4	3.8	3.4	0.83	19.2	4.7	2.6	0.86	42.5	4.4	4.2
0.70	18.1	3.6	3.1	0.75	18.2	4.1	2.4	0.79	40.0	3.8	3.8
0.60	16.8	3.2	2.6	0.67	22.2	5.1	3.0	0.71	41.0	3.8	3.7
0.50	15.6	3.2	2.4	0.58	23.5	4.9	2.9	0.64	38.3	3.5	3.7
0.40	14.4	3.4	2.2	0.50	25.2	4.6	2.8	0.57	32.6	3.4	3.6
0.30	13.2	3.0	1.8	0.42	19.7	4.8	2.7	0.50	30.1	3.6	3.8
0.20	11.9	2.8	1.7	0.33	16.6	3.8	2.1	0.43	30.2	3.6	3.8
0.10	10.7	2.8	1.7	0.25	15.4	3.7	2.0	0.36	27.5	3.6	3.7
0.00	9.5	2.8	1.8	0.17	14.1	3.8	2.0	0.29	27.3	3.6	3.8
				0.08	17.2	4.1	2.2	0.21	27.0	3.6	3.6
				0.00	15.5	4.3	2.2	0.14	23.8	4.0	4.0
								0.07	20.5	4.6	4.2
								0.00	19.3	4.6	4.2

isometrically at 0% (anterior b = 0.2, 95%CI −0.4 to 0.6; posterior b = 0.2, 95%CI -0.4 to 0.8), 50% (anterior b = −0.1, 95%CI −0.7 to 0.3; posterior b = −0.1 95%CI −0.8 to 0.5), and 100% maximal gape (anterior b = 0.2, 95%CI −0.6 to 0.9; posterior b =0.0, 95% CI −0.7 to 0.8).

Stimulated bite forces for six individuals (taken with the mouth approximately 30% maximum gape) were not significantly different ($P > 0.05$) from theoretical bite force values taken at the anterior bite point for the same individuals at 0% and 50% maximal gape, but were larger than bite force estimated at 100% maximal gape (Fig. 7).

Strike Dynamics

Maximum velocity of the king mackerel ranged from 3.3 to 15.8 bl/s (8.5 ± 4.9 SD) and maximum initial acceleration of the prey ranged from 0.5 to 12.8 m/s^2 (7.7 ± 4.9 SD) (Table 2). Force applied to the prey ranged from 0.1 to 1.9 N (1.2 ± 0.7 SD) while maximum predator force of the king mackerel ranged from 2.1 to 81.6 N (35. 7 ± 27.5 SD) (Table 2).

Bite pressure

Jaw position had a significant effect ($P < 0.05$) on bite pressure in the smallest and largest fish, with higher pressures toward the back of the jaw. Maximum bite pressures were 18.1 MPa, 25.2 MPa, and 56.9 MPa for the small, medium and large fish, respectively. Tooth depth had a significant effect ($P < 0.001$) on bite pressure for all three fish, with higher pressure when 10% (tip) of the tooth was penetrated and lower pressure at 50% and the lowest pressure at 100% (Fig. 8, Table 3).

Comparison Among Other Fishes

There was a significant positive relationship between bite force and mass for 20 species of teleost fishes and sharks (Log ABF = 0.507 log mass + 0.729, $r^2 = 0.565$, $t = 4.83$, $P < 0.001$). This relationship remained after performing a phylogenetically-corrected regression (Log ABF = 0.576 log mass + 0.288, McFadden's pseudo-$r^2 = 0.247$, t = 6.21, $P < 0.001$). When ranking fish on mass-specific bite force, the King mackerel had the second lowest force based on conventional residuals, and the second lowest force based on phylogenetic residuals (Table 4).

DISCUSSION

Bite Force

A better understanding of feeding performance is likely to be gained by simultaneously considering multiple performance parameters during feeding events. The results of this study indicate that king mackerel generate relatively low biting and

Table 4. Values of anterior bite force (ABF) for 20 species of teleost and cartilaginous fishes obtained from the literature. Studentized residuals are from a linear regression of log ABF against log mass, as well as phylogenetic residuals based on Revell (2009).

Species name	Common name	ABF (N)	Mass (g)	Residuals	Phylogenetic residuals
Chilomycterus schoepfi[a]	striped burrfish	380	180	2.576	2.658
Lachnolaimus maximus[b]	hogfish	290	209	2.230	2.302
Archosargus probatocephalus[c]	sheepshead	309	998	1.500	1.464
Heptranchias perlo[d]	sharpnose sevengill shark	245	1614	1.024	0.955
Heterodontus francisci[e]	horn shark	206	2948	0.545	0.435
Hydrolagus colliei[f]	whitespot chimaera	106	870	0.499	0.474
Sphyrna mokarran[g]	great hammerhead shark	2432	580598	0.333	−0.142
Carcharhinus limbatus[h]	blacktip shark	423	22092	0.242	−0.007
Halichoeres maculipinna[b]	clown wrasse	11	18	0.202	0.443
Carcharhinus leucas[g]	bull shark	1023	140341	0.187	−0.189
Chiloscyllium plagiosum[d]	whitespotted bambooshark	93	1219	0.198	0.148
Negaprion brevirostris[d]	lemon shark	79	1219	0.035	−0.015
Halichoeres garnoti[b]	yellow head wrasse	10	21	0.029	0.259
Thalassoma bifasciatum[b]	bluehead wrasse	5	7	−0.107	0.199
Halichoeres bivittatus[b]	slippery dick	5	19	−0.614	−0.376
Sphyraena barracuda[i]	great barracuda	83	11900	−1.072	−1.279
Squalus acanthias[j]	piked dogfish	19.6	1065	−1.291	−1.33
Etmopterus lucifer[d]	blackbelly lanternshark	3.1	48	−1.562	−1.388
Scomberomorus cavalla	king mackerel	44.58	12684	−1.726	−1.937
Etmopterus spinax[d]	velvet belly lanternshark	1.6	349.1	−3.230	−3.193

[a]Korff & Wainwright (2004).
[b]Clifton & Motta (1998).
[c]Hernandez & Motta (1997).
[d]Huber (2006).
[e]Huber et al. (2005).
[f]Huber et al. (2008).
[g]Huber & Mara (unpubl. data).
[h]Huber et al. (2006).
[i]Habegger et al. (2010).
[j]Huber & Motta (2004).

prey forces while striking at high velocities with high tooth pressures. The mechanical advantage of the king mackerel lower jaw adducting mechanism scaled with isometry at all gape angles. Its anterior mechanical advantage (0.18–0.21) is considered intermediate amongst fishes (Westneat, 2004), resulting in a speed-efficient jaw with relatively inefficient transfer of force from the musculature to the prey. Mechanical advantage at the posterior (0.62–0.77) bite point results in a more efficient transmission of force than at the anterior bite point. Variation in the posterior MA may be due to error during digitizing of the posterior bite point, as the last tooth position was variable and difficult to ascertain. Most piscivorous fish rely on speed efficient jaws (low MA) rather than force efficient jaws (high MA) in order to capture elusive prey (Westneat, 2004). The great barracuda, *Spyraena barracuda*, which consumes similar prey to the king mackerel, has an average anteriror MA of 0.27 (Habegger et al., 2010). However the durophagous horn shark, *Heterodontus francisci*, has an anterior MA of 0.50 and posterior MA of 1.06, in which the resultant bite force exceeds the force generated by the adductive musculature (Huber et al., 2005).

Bite force of king mackerel scaled isometrically with respect to body size at all gape angles for these adult king mackerel (Fig. 6), despite positive allometry of adductor mandibulae CSA. This apparent discrepancy may be due large variability in the MA that masks the positive allometry seen in the CSA of the adductor complex, resulting in isometry of bite force values. In contrast, the bite force of the bull shark, *Carcharhinus leucas*, scaled with positive allometry for juveniles and with isometry for adults (Habegger et al., 2012). This pattern suggests that it may be important for juveniles to rapidly develop high bite forces in order to exploit prey resources, but that the large size and absolute bite forces of adults alleviates the need for allometric

performance. More work is needed to examine if differential scaling exists between juvenile and adult king mackerel, although high bite pressures (see below) may alleviate the need for allometric increases in bite force at early life history stages. Interestingly, king mackerel had the second lowest anterior mass-specific bite force (Table 4) of 20 species of bony and cartilaginous fish, with only the velvet belly lanternshark, *Etmopterus spinax,* producing a lower mass-specific bite force (Huber et al., 2009). These findings suggest that high bite forces are not necessary for effective predation by king mackerel.

Stimulated bite force (taken at the anterior jaw), at approximately 30% of maximum gape, was not significantly different ($P = 0.056$) than the theoretical anterior bite force estimated at 0% and 50% maximum gape, although marginal significance and low sample size indicates the stimulated bite force might be greater, suggesting that the 3D-static equilibrium model used to estimate bite force is representative of actual tetanic bite force for this species, corroborating the results of Huber et al. (2005) and Mara et al. (2010). Stimulated bite force was larger than theoretical bite force at 100% maximal gape because the theoretical bite force was the lowest when the gape was maximally open. Accounting for gape in quantification of bite force is essential because motion of the jaw affects length-tension relationships of muscles, insertion angles of tendons, and changes in leverage. Numerous studies have found maximum bite forces at intermediate gape angles (Williams et al., 2009; Chrsitiansen, 2011; Gidmark et al., 2013). For example, Williams et al. (2009) found that the bite force of rodents peaked at approximately 40% of maximum gape and Ferrara et al. (2011) found that white sharks, *Carcharodon carcharias*, have higher bite forces at a gape angle of 35° (mouth open, 1602 N) than 0° (mouth closed, 1303 N) because a unique attribute of the primary jaw adductor (mid-lateral raphe) allows reorientation of muscle fibers during mouth opening. Unlike these studies, king mackerel bite force was inversely proportional to gape angle, which has also been observed among bat species (Dumont et al., 2003).

The limited amount of volume within the vertebrate head may result in an evolutionary compromise, such as spatial trade-offs on adjacent body structures or size of the constituent parts (Hulsey et al., 2007). In some cichlids (Cichlidae) the suspensorium and adductor muscles may be reduced by large eye size (Barel, '83; Hulsey et al., 2007). In the case of king mackerel, low bite force may be a result of a hydrodynamic trade off in that streamlining of the body selects against large jaw adductor muscles, thereby constraining bite force (Herrel et al., 2001, 2002). Boundary layer separation can be delayed, resulting in reduced pressure drag when the widest plane of the fish is further back on the body (Walters, '62). The widest plane of the king mackerel occurs near the operculum, just posterior to the jaw adductors. Thus, having higher biting forces and the necessary large jaw adductor muscles (Herrel et al., 2001) could hinder swimming performance of king mackerel, thereby compromising the speed of their strike. In the bull shark, *Carcharhinus leucas*, head width is positively correlated to bite force, and this shark generates the highest mass specific bite force of any shark measured to date (Habegger et al., 2012). Based on comparative head geometry and bite forces, it therefore appears that large ram-feeding predators occupy this niche by virtue of selection for disparate parameters.

Strike Dynamics

King mackerel attain high strike velocities (15.8 bl/s, Table 2) resulting in forward forces being exerted on their prey during ram feeding. However, forces experienced by prey (1.9 N, Table 2) were considerably smaller than those generated by the predator because of the relative masses of the king mackerel and the smaller prey fish; only a small fraction of the predator force is actually applied to the prey item, whereas a prey of larger mass would experience a larger fraction of the predator force. Furthermore, forces experienced by prey due to the forward motion of the predator were also considerably lower than bite forces. Nonetheless, high speeds may be important for surprising and chasing down elusive prey. Walters ('62) estimated a conservative swimming speed of scombroid fishes to be approximately 10 bl/s, with other studies documenting peak swimming speeds of 13.4 bl/s in the bluefin tuna, *Thunnus thynnus*, and 11.0 bl/s in the Atlantic mackerel, *Scomber scombrus* (Lane, '41; Videler and Hess, '84). Aquarium-housed juvenile great barracuda were reported to strike prey at 7.5 bl/s, although this was likely submaximal performance (Porter and Motta, 2004). Similar to other scombroids, king mackerel benefit from high swimming speeds in their ability to successfully chase down and capture elusive prey.

Bite Pressure

The generation of high bite pressures facilitates the consumption of soft-bodied prey and likely alleviates any perceived performance deficiency attributed to low bite or prey forces. For example, the sharp teeth of sharks require very little force to penetrate prey such as ladyfish, *Elops saurus* (mean 6.7 ± 1.3 N), and white grunt, *Haemulon plumieri* (mean 10.9 ± 2.1N) owing to high pressures generated during biting (Whitenack and Motta, 2010). King mackerel are able to produce bite pressures upwards of 57 MPa (Fig. 8, Table 3), which is consistent with other piscivorous vertebrates. In fact, piscivorous crocodilian with low bite forces are capable of generating bite pressures of upwards of 1344 MPa (Anderson and Westneat, 2006; Erickson et al., 2012). The bite pressure of king mackerel was highest at the posterior jaw when only the tip of the tooth was penetrating the prey (Fig. 8) and decreased greatly as tooth penetration depth increased. As bite pressure is greatest posteriorly, while tooth size increases posteriorly and worn teeth are readily replaced to maintain a sharp cutting surface (Morgan and King, '83), it may be advantageous to strike and/or bite prey at this posterior region.

This finding is consistent with the observation of bite marks from failed captures on bait. The gape must be at a large angle in order for prey to reach the rear of the mouth, a jaw position that results in lower bite force, suggesting again that bite pressure may play a more important role in feeding than absolute bite force.

It is unknown whether or not prey contact due to jaw closure, and forward motion of the predator, occurs at the same instant. If these two events are instantaneous, the resultant forces on the prey may be additive. Because the prey size is small relative to the king mackerel, the predator force would contribute little to overall feeding success and bite forces/pressures dominate the predator-prey interaction. High-speed kinematic studies of striking great barracuda (Porter and Motta, 2004) suggest that these two events occur at the same time, although kinematic analyses of king mackerel feedings are needed to elucidate this relationship.

CONCLUSIONS

King mackerel, *Scomberomorus cavalla*, have relatively low performance for bite force compared with other fishes and relatively little of the forward predator force is experienced by the prey. However, king mackerel can attain high swimming speeds to chase prey and use sharp teeth to impart high bite pressure, factors which apparently alleviate the need for high bite forces.

ACKNOWLEDGMENTS

We would like to thank many people and institutions that contributed to this study. We thank S. Deban for his suggestions and comments.. Many thanks to Captain D. Zalewski, Captain P. Tedrick, A. Schilling, and K. Ecker for help with collecting specimens and data. Thanks to H. Ferguson, L. Habegger, C. Stinson, and J. Brown for their feedback and advice. Special thanks to H. Ferguson for construction of fishing reel camera mounts. This study was supported in part by the Porter Family Foundation and the Guy Harvey Ocean Foundation to ARF.

LITERATURE CITED

Anderson PS, Westneat MW. 2006. Feeding mechanics and bite force modeling of the skull of *Dunkleosteus terrelli*, an ancient apex predator. Biol Lett 3:76–79.

Bainbridge R. 1960. Speed and stamina in three fish. J Exp Biol 37:129–153.

Barel CDN. 1983. Form-relations in the context of constructional morphology: the eye and suspensorium of lacustrine Cichlidae (Pisces, *Teleostei*). Neth J Zool 34:439–502.

Betancur R, Broughton RE, Wiley EO, et al. 2013. The tree of life and a new classification of bony fishes. PLOS Curr 5.

Bernal D, Dickson KA, Shadwick RE, Graham JB. 2001. Review: analysis of the evolutionary convergence for high performance swimming in lamnid sharks and tunas. Comp Biochem Physiol A: Mol Integr Physiol 129:695–726.

Clifton KB, Motta PJ. 1998. Feeding morphology, diet and ecomorphological relationships among five Caribbean labrids (Teleostei, Labridae). Copeia 1998:953–966.

Dumont ER, Herrel A. 2003. The effects of gape angle and bite point on bite force in bats. J Exp Biol 206:2117–2123.

Erickson GM, Lappin AK, Vliet KA. 2003. The ontogeny of bite-force performance in in American alligator (*Alligator mississippiensis*). J Zool Lond 260:317–327.

Erickson GM, Gignac PM, Steppan SJ, et al. 2012. Insights into the ecology and evolutionary success of crocodilians revealed through bite-force and tooth-pressure experimentation. PloS One 7: e31781.

Ferrara TL, Clausen P, Huber DR, et al. 2011. Force versus speed: mechanics of biting in great white and sandtiger sharks. J Biomech 44:430–435.

Gidmark NJ, Konow N, LoPresti E, Brainerd EL. 2013. Bite force is limited by the force-length relationship of skeletal muscle in black carp, *Mylopharyngodon piceus*. Biol Lett 9:2012–1181.

Grafen A. 1989. The phylogenetic regression. Philos Trans R Soc B 326:119–157.

Grubich JR, Rice AN, Westneat MW. 2008. Functional morphology of bite mechanics in the great barracuda (*Sphyraena barracuda*). J Zool 111:16–29.

Habegger ML, Motta PJ, Huber DR, Deban SM. 2010. Feeding biomechanics in the great barracuda during ontogeny. J Zool 283:63–72.

Habegger ML, Motta PJ, Huber DR, Dean MN. 2012. Feeding biomechanics and theoretical calculations of bite force in bull sharks (*Carcharhinus leucas*) during ontogeny. J Zool 115:354–364.

Heinicke MP, Naylor JP, Hedges SB. 2009. Cartilaginous fishes (Chondrichthyes). In: Hedges SB, Kumar S. editors. The timetree of life. New York: Oxford University Press. p 320–327.

Herrel A, Grauw ED, Lemos-Espinal JA. 2001. Head shape and bite performance in Xenosaurid Lizards. J Exp Zool 290:101–107.

Herrel A, Adriaens D, Verraes W, Aerts P. 2002. Bite performance in clariid fishes with hypertrophied jaw adductors as deduced by bite modeling. J Morphol 253:196–205.

Herrel A, Van Wassenbergh S, Wouters S, Aerts P, Adriaens D. 2005. A functional morphological approach to the scaling of the feeding system in the African catfish, Clarias gariepinus. J Exp Biol 208:2091–2102.

Herrel A, Holanova V. 2008. Cranial morphology and bite force in *Chamaeleolis* lizards, adaptations to molluscivory? J Zool 111:467–475.

Hernandez LP, Motta PJ. 1997. Trophic consequences of differential performance: ontogeny of oral jaw crushing performance in the sheepshead, *Archosargus probatocephalus* (Teleostei: Sparidae). J Zool 243:737–756.

Higham TE, Day SW, Wainwright PC. 2005. Sucking while swimming: evaluating the effects of ram speed on suction generation in bluegill sunfish Lepomis macrochirus using digital particle image velocimetry. J Exp Biol 208:2653–2660.

Holzman R, Collar DC, Mehta RS, Wainwright PC. 2012. An integrative modeling approach to elucidate suction-feeding performance. J Exp Bio 215:1–13.

Huber DR2006. Cranial biomechanics and feeding performance of sharks. PhD dissertation, University of South Florida, Tampa, FL, USA.

Huber DR, Motta PJ. 2004. Comparative analysis of methods for determining bite force in the spiny dogfish *Squalus acanthias*. J Exp Zool 301:26–37.

Huber DR, Eason TG, Hueter RE, Motta PJ. 2005. Analysis of the bite force and mechanical design of the feeding mechanism of the durophagous horn shark *Heterodontus francisci*. J Exp Biol 208:3553–3571.

Huber DR, Weggelaar CL, Motta PJ. 2006. Scaling of bite force in the blacktip shark *Carcharhinus limbatus*. J Zool 109:109–119.

Huber DR, Dean MN, Summers AP. 2008. Hard prey, soft jaws and the ontogeny of feeding mechanics in the spotted ratfish *Hydrolagus colliei*. J Roy Soc Int 5:1–12.

Hulsey CD, Mims MC, Streelman JT. 2007. Do constructional constraints influence cichlid craniofacial diversification?. Proc R Soc B 274:1867–1875.

Kolmann MA, Huber DR. 2009. Scaling of feeding biomechanics in the horn shark *Heterodontus francisci*: ontogenetic constraints on durophagy. J Zool 112:351–361.

Korff WL, Wainwright PC. 2004. Motor pattern control for increasing crushing force in the striped burrfish (*Chilomycterus schoepfi*). J Zool 107:335–346.

Lailvaux SP, Herrel A, VanHoodonch B, Meyers JJ, Irschick DJ. 2004. Performance capacity, fighting tactics and the evolution of life-stage male morphs in the green anole lizard (*Anolis carolinensis*). Proc R Soc Lond B 271:2501–2508.

Lane FW. 1941. How fast do fish swim? Country Life 534–535.

Lajeunesse MJ, Fox GA. 2015. Statistical approaches to the problem of phylogenetically correlated data. In: Fox GA, Negrete-Yankelevitch S, Sosa VJ, editors. Ecological statistics: contemporary theory and application. Oxford, UK: Oxford University Press. p 262–284.

Lauder GV. 1980. The suction feeding mechanism in sunfishes (*Lepomis*): an experimental analysis. J Exp Biol 88:49–72.

Mara KR, Motta PJ, Huber DR. 2009. Bite force and performance in the durophagous bonnethead shark, *Sphyrna tiburo*. J Exp Zool 313:95–105.

McCormick MI, Molony BI. 1993. Quality of the reef fish *Upeneus tragula* (Mullidae) at settlement: is size a good indicator of condition? Mar Ecol Prog Ser 98:45–54.

Morgan EC, King WK. 1983. Tooth replacement in king mackerel, *Scomberomorus cavalla*. (Pieces: Scombridae). Southwest Nat 28:261–269.

Norton SF. 1991. Capture success and diet of cottid fishes: the role of predator morphology and attack kinematics. Ecology 72:1807–1819.

Paradis E, Claude J, Strimmer K. 2004. APE: an R package for analyses of phylogenetics and evolution. Bioinformatics 20:289–290.

Pinheiro J, Bates D, DebRoy S, Sarkar D and the R Core team. 2015. nlme: linear and nonlinear mixed effects models. R package version 3.1-120. http://cran.r-project.org/ web/packages/nlme/index.html

Pohlmann K, Grasso FW, Breithaupt T. 2001. Tracking wakes: the nocturnal predatory strategy of piscivorous catfish. PNAS 98:7371–7374.

Porter HT, Motta PJ. 2004. A comparison of strike and prey capture kinematics of three species of piscivorous fishes: Florida gar (*Lepisosteus platyrhincus*), redfin needlefish (*Strongylura notata),* and great barracuda (*Sphyraena barracuda*). Mar Biol 145:989–1000.

Revell LJ. 2009. Size-correction and principal components for interspecific comparative studies. Evolution 63:3258–3268.

Revell LJ. 2012. Phytools: an R package for phylogenetic comparative biology (and other things). Methods Ecol Evol 3:217–223.

Rice AN, Westneat MW. 2005. Coordination of feeding, locomotion, and visual systems in parrotfishes (Teleostei: Labridae). J Exp Biol 208:3503–3518.

Rohlf FJ. 2001. Comparative methods for the analysis of continuous variables: geometric interpretations. Evolution 55:2143–2160.

Schaerlaeken V, Holanova V, Boistel R, et al. 2012. Built to bite: feeding kinematics, bite forces and head shape of a specialized durophagous lizard, *Dracaena guianensis* (Teiidae). J Exp Zool 317A:371–381.

SEDAR 2009. SEDAR 16-Complete stock assessment report: South Atlantic and Gulf of Mexico, Mexico king mackerel. Southeast Data Assessment and Review, North Charleston, SC.

Shashar N, Hagan R, Boal JG, Hanlon RT. 2000. Cuttlefish use polarization sensitivity in predation on silvery fish. Vision Res 40:71–75.

Stewart WJ, Cardenas GS, McHenry MJ. 2013. Zebrafish larvae evade predators by sensing water flow. J Exp Zool 216:388–398.

Van Wassenbergh S, Herrel A, James RS, Aerts P. 2007. Scaling of contractile properties of catfish feeding muscles. J Exp Biol 210:1183–1193.

Veall MR, Zimmermann KF. 1996. Pseudo-R2 measures for some common limited dependent variable models. J Econ Surv 10:241–259.

Vélez-Zuazo X, Agnarsson I. 2011. Shark tales: a molecular species-level phylogeny of sharks (Selachimorpha, Chondrichthyes). Mol Phylogenet Evol 58:207–217.

Videler JJ, Hess F. 1984. Fast continuous swimming of two pelagic predators, saithe (*Pollachius virens*) and mackerel (*Scomber scombrus*): a kinematic analysis. J Exp Biol 109:209–228.

Walters V. 1962. Body form and swimming performance in the scombroid fishes. Am Zool 2:143–149.

Wainwright PC. 1988. Morphology and ecology: functional basis of feeding constraints in Caribbean labrid fishes. Ecology 69:635–645.

Wainwright PC. 1991. Ecomorphology: experimental functional anatomy for ecological problems. Am Zool 31:680–693.

Wainwright PC, Ferry-Graham LA, Waltzek TB, et al. 2001. Evaluating the use of ram and suction during prey capture by cichlid fishes. J Exp Biol 204:3039–3051.

Wall CC, Muller-Karger FE, Roffer MA. 2009. Linkages between environmental conditions and recreational king mackerel (*Scomberomorus cavalla*) catch off west-central Florida. Fisheries Oceanography 18:185–199.

Westneat MW. 2004. Evolution of levers and linkages in the feeding mechanics of fishes. Int Comp Biol 44:378–389.

Whitenack LB, Motta PJ. 2010. Performance of shark teeth during puncture and draw: implications for the mechanics of cutting. Biol J Linn Soc 100:271–286.

Whitenack LB, Simkins DC, Jr, Motta PJ. 2011. Biology meets engineering: the structural mechanics of fossil and extant shark teeth. J Morphol 272:169–179.

Wilga CD, Motta PJ. 1998. Conservation and variation in feeding mechanism of the spiny dogfish *Squalus acanthias*. J Exp Biol 201:1345–1358.

Williams SH, Peiffer E, Ford S. 2009. Gape and bite force in the rodents *Onychomys leucogaster* and *Peromyscus maniculatus*: does jaw-muscle anatomy predict performance? J Morphol 270:1338–1347.

Winterbottom R. 1974. A descriptive synonymy of the striated muscles of the Teleostei. Proc Acad Nat Sci Phila 125:225–317.

Wroe S, Huber DR, Lowry M, et al. 2008. Three-dimensional computer analysis of white shark jaw mechanics: how hard can a great white bite? J Zool 276:34–336.